The stochastic structure of oil prices: modelling, Monte Carlo simulations and value at risk estimates

Leopoldo Grajeda, José Roberto Steiner, Raphael Lima

Department of Research and Development, GAVB Consulting (Boticario Group)
Rua São Pedro, 440 – Marechal Rondom. 92020-480 Canoas, RS – Brazil

A R T I C L E I N F O

Article history:
Final version 3 March 2022

Keywords:
Oil prices
Black–Scholes
Volatility models
Models with jumps
Monte Carlo methods
Value at risk

Classification:
JEL: C150, C630, G130, G170, Q310

A B S T R A C T

This work models crude oil prices as an Itô process imbued with a periodic deterministic term. A generalized Black–Scholes stochastic differential equation is introduced, with adaptive parameters. Historic monthly data from July 2007 to July 2021 are used to compute these parameters through a standard monthly time series analysis, and then daily data are used to further refine the trend and volatility terms of the decomposition. The proposed model for Brent contracts was validated with market data, allowing for an improved understanding of the stochastic structure of oil prices, as well as for better estimates of stochastic volatility and return. As an illustration of possible applications, Markov Chain Monte Carlo simulations for oil prices were built and used to estimate value at risk for a physical hedging operation.

1. Introduction

In his breakthrough work [1], Bachelier already pointed out that, although the market dynamics will never be an exact science, a statistical treatment of prices' variations is suitable. In his pioneering masterpiece of modern Finance, he treated options on commodities trading on a mercantile exchange. Unfortunately, despite his amazing insight about market structure, the mathematical framework needed to implement his ideas was not fully available at that time. Indeed, the toolbox of stochastic calculus just started to be devised a few years later, after Einstein's classic work on Brownian motion [2], and became fully operational only about half a century later, with the framework built by Itô [3].

A couple of decades after Itô laid the foundations of modern stochastic calculus, the ideas envisioned by Bachelier finally produced outstanding results in Finance with Black and Scholes' work [4]. Their model's underlying premise is that a stock price S_t follows a geometric Brownian motion, with two constant parameters: expected return μ and volatility σ, estimated originally as mean and standard deviation of the relative return, respectively. The corresponding Itô stochastic process follows the differential equation

$$\frac{dS}{S} = \mu\, dt + \sigma\, \eta\, \sqrt{dt}\,, \tag{1}$$

where the noise η follows the standard normal distribution. Then, a clever usage of arbitrage theory, combined with Itô's lemma, was made to cancel out the stochastic component of equation (1) and thus obtain a usual parabolic partial differential equation of second order for the pricing of derivatives. The resulting equation was then solved by traditional techniques of advanced calculus, leading to their formulae for pricing European options on stocks [4]. That was the cornerstone of continuous time financial theory and gave birth to several applications to risk analysis, such as pricing and hedging of futures and derivatives.

Numerous variations on the same theme were successfully made over the last five decades, with much criticism about how well, or how bad, Black–Scholes model performs in market applications. On the critics' side, it is important to mention the work of Haug and Taleb, that points out that, in practice, most traders still prefer traditional tools that existed far earlier, rather than any of the Black–Scholes model's advanced variations [5]. Indeed, constant parameters in equation (1) render it useless on the long run. In practice, both expectations and volatility vary a lot over time, sometimes even with abrupt jumps, so that both expected return μ and volatility σ, if assumed to be constant, must be recomputed quite often to keep up with market data.

A priori, that would not be a problem for derivative traders, as most options and futures usually have short maturities. However, since

$$\lim_{\Delta t \to 0} \frac{\sqrt{\Delta t}}{\Delta t} = \infty, \tag{2}$$

the stochastic component over small Δt in equation (1) is far larger than the deterministic one, so that that Black–Scholes analysis is useless for high frequency traders or day traders, and of little practical application for users of short-term instruments. Moreover, to implement the model's most advanced

variations, made to close the gap on reality, one needs both a deep understanding of stochastic calculus and a huge computational effort, making the everyday use of them mostly unpractical.

Of course, as stochastic calculus becomes more popular, computing gets cheaper and faster, and artificial intelligence techniques advance, the most sophisticated, improved variations of Black–Scholes model are gradually making their way to the traders' desks, especially for mid- and long-term operations. As the consequences of equation (2) cannot be easily overcome, the short-term applications of the model remain a challenge for traders and analysts.

In spite of its little practical application in the early 1970's, Black–Scholes model is philosophically sound, insightful and beautiful, so that, by the turn of that decade, many upgraded versions had already shown up, precisely to deal with traders' founded concerns. To name just a few such major works, scholars like Merton considered stock returns with jumps [6], while other authors such as Hull and White dealt with stochastic volatility [7]. Anyway, ever since Black and Scholes succeeded in explaining the pricing of options on blue chips, numerous attempts have been made either to improve the model for other stocks or to build similar ones for other kinds of assets, such as the works of Garman and Kohlhagen [8] or Heston [9] for options on currency.

Naturally, there were many such attempts to apply Black–Scholes model to commodities, for instance the work of Cox, Ingersoll Jr. and Ross [10], which addressed commodities in general, but not dealing with any specific asset. That approach was relatively successful for gold, as noted by Beckers [11], for which market is quite efficient and both production and consumption are negligible. Overall, gold prices are driven mostly by market expectations alone, quite in the same way as blue chips' prices are, with follow on public offers set aside.

In special for oil future contracts and options, however, despite of its theoretical soundness and insight, in practice, most similar attempts to apply Black–Scholes model have consistently failed on the long run, as pointed out by Schwartz [12]. As stock prices, or almost any prices, oils prices are driven mostly by market forces: supply and demand. Nevertheless, unlike stocks and even though oil will eventually run out, oil supply seems to be virtually unlimited in the foreseeable future, with production adjusted, at a cost, to match demand, as it can be seen on the yearly report on energy by bp™ [13]. Storage fees and convenience yields also play important roles and, on the other hand, demand is not led only by market expectations and global economic growth, but also and mostly by consumption, which has a distinct seasonal character, as shown by Hunt and Ninomiya [14], for instance. Other peculiar features of oil markets and their impacts on prices are explored in detail by many scholars like Pindyck [15], Hamilton [16], Kolodziej and others [17] and Byun [18].

Seasonal variations in the oil market are not accounted by the geometric Brownian motion of equation (1), nor by its standard variations, which usually sweep this seasonal behavior under the stochastic term carpet. Although the periodic component has null average and is relatively small in comparison to the stochastic component, this practice may unnecessarily increase the volatility and imbue the stochastic volatility with a seasonal behavior, as indeed pointed out by Arismendi and others [19]. This alters the probability distribution of the random component and makes it difficult to deal with, thus ruining the model precision on the long run and limiting its use for traders and investors.

This work further details the stochastic structure of oil prices devised by Schwartz and validates the proposed model with Brent oil market data. It improves on previous variations of Black–Scholes model by taking the seasonality of oil markets into the deterministic component of the Brownian motion,

which allows for a better decomposition of the prices' time series. Next, a volatility ratio is used to establish the lognormal structure of the stochastic volatility and the stochastic structure of the non-seasonal trend of the expected return is also explored. Finally, in order to illustrate the possible applications of the proposed and validated stochastic structure of Brent oil prices, the parameters estimated here are used to produce some Markov Chain Monte Carlo simulations, which are then used to obtain value at risk estimations for a hedger with a long position, considering physical storage fees.

2. Market data

2.1. Positive prices

Black–Scholes equation (1) implicitly relies on positive prices. In general, the assumption that $S > 0$ makes sense for stocks, as well as for any good that can be easily disposed of. However, as recently seen in the American oil market, WTI contracts have indeed traded at negative prices in April 2020, as oil could not be simply dumped away when most American traders' storage capacity was exhausted.

Although many scholars have resorted back to Bachelier's model, such as Choi and others [20], this market condition is so rare and so extreme that, despite its academic relevance, having a good model for it is rather useless for market practitioners. Moreover, even in the most severe of market conditions, world's storage capacity is far larger than that of one country alone, so that Brent oil prices also suffered along the COVID-19 crisis but remained positive so far. Thus, this work deals only with prices of Brent contracts, since the model developed here generalizes equation (1) and therefore also relies on positive prices.

2.2. Market data retrieval

As for the market data considered, this work is based exclusively on data publicly available over the Internet. The historic crude oil price series was taken as the daily close price for the shortest maturity futures contract at New York Mercantile Exchange, used as a proxy for the oil spot prices. The data was retrieved from Yahoo! Finance API [21], both for Brent and WTI futures, from 07/31/2007 to 07/31/2021. The prices are all in dollars per oil barrel[*], the oil market standard for trading quotes. FIGURE 1 shows the Brent oil daily close price proxy considered. It is easy to perceive the stochastic behavior of oil prices, as the graph is all but smooth.

[*] A barrel is a non-SI volume unit, which appears in several different contexts and may range from 100 L to 200 L. In the crude oil market, 1 bbl = 158.99 L.

FIGURE 1: Brent future's daily close prices, from 07/31/2007 to 07/31/2021. Source: Yahoo! Finance.

A few remarkable features of the Brent prices time series can also be seen in FIGURE 1, for instance, the all-time high daily close price of 144.97 USD / bbl. on July 11, 2008, or the effect of some major worldwide economic crises, such as the subprime crisis of 2008 and the COVID-19 crisis of 2020, and the respective ensuing recoveries.

2.3. Data preprocessing

All data preprocessing and most calculations were made in Python. To begin with, days with missing data were dropped from the database and the relative daily return was computed for each trading day. As a monthly time scale will be mostly used throughout this work, the data was then filtered to a monthly close price series, taking P_t as the close price of the last day of month t. The price P_t was used to directly compute the corresponding relative return r_t of each month as

$$r_t = \frac{\Delta P_t}{P_{t-1}} = \frac{P_t}{P_{t-1}} - 1 \tag{3}$$

The resulting monthly relative returns, from August 2007 to July 2021, are shown on FIGURE 2:

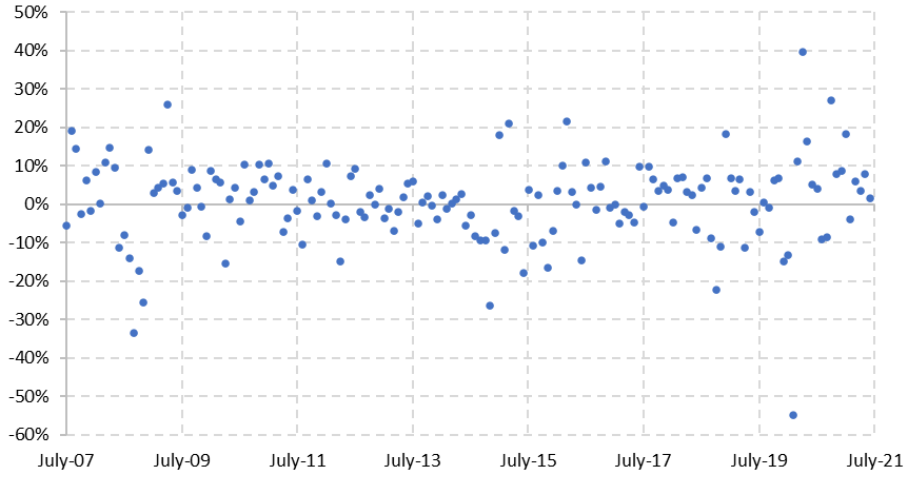

FIGURE 2: Relative monthly returns of Brent prices, from August 2007 to July 2021.

Note that outliers can be easily spotted in FIGURE 2, such as those huge negative and positive relative monthly returns concerning the subprime and COVID-19 crises. In data science, those outliers would usually be disregarded; nevertheless, those extreme returns may result in huge financial losses or gains, and therefore cannot be simply ignored. In Finance, every single monthly relative return must be properly accounted for.

3. Modelling and methodology

3.1. Modelling the oil price stochastic process

This work proposes a model that considers P_t, the spot price of oil at the end of month t, to follow a Lévy process with a stochastic differential equation of the form:

$$\frac{dP}{P} = [\mu(t) + \lambda(t)]\, dt + \xi \sqrt{dt} \tag{4}$$

Here, the deterministic component of the instantaneous relative rate of change is modelled by a non-periodic trend $\mu(t)$ and an additional seasonal term $\lambda(t)$, while the stochastic component is generalized to a noise ξ that follows a stable distribution with mean 0. Since the Lévy alpha-stable distribution family includes the Gaussian, this equation directly generalizes equation (1). Indeed, if $\mu(t)$ is constant, $\lambda(t) \equiv 0$ and $\xi = \sigma\, \eta$ follows a normal distribution, equation (4) reduces to equation (1), the usual geometric Brownian motion of traditional Black–Scholes model.

In the proposed model, $\mu(t)$ captures the market expectations, which are determined by economic and populational growth, oil consumption habits, interest rates and other factors usually referred to as

the commodity super-cycle. All those factors do vary over time, possibly with jumps, and the variation of this term not only allows the model to better fit the oil super-cycle market expectations, but also to adjust to bull or bear market scenarios as well, when the market as a whole expects sustained increases or decreases in price, respectively. On its turn, $\lambda(t)$ detects the seasonal variation in oil consumption, such as the need of heating oil every winter or the power usage for industrial production cycles.

As for the stochastic component, given the characteristics of the global oil market, ξ is expected, but not required, to be close a white noise. The volatility itself is also not required to be constant, nor smooth, not even explicitly defined. As any trader knows from heart, volatility does indeed vary a lot over time, as markets get more "nervous" from time to time, especially due to factors such as political unrests and wars in major oil producing countries or economic crises, among other possible sources of increased uncertainty.

3.2. Time series analysis of the monthly returns

The monthly returns must then be adjusted into the differences' equation corresponding to equation (4), namely

$$\frac{\Delta P}{P} \approx [\mu(t) + \lambda(t)]\,\Delta t + \xi\sqrt{\Delta t} \tag{5}$$

As time is measured in months, by taking $\Delta t = 1$, equation (5) reduces further to

$$\frac{\Delta P}{P} \doteq \mu(t) + \lambda(t) + \xi \tag{6}$$

In order to fit the monthly returns' time series data into equation (6), a straightforward additive seasonal decomposition was made, with a 12-month centered moving average filtering, using the function available on Statsmodels Python library [22]. Due to this smoothing, the period considered in this work was further limited to a time span of 13 complete years, from March 2008 to February 2021. The results are exhibited on Section 4.1.

Once the monthly returns' time series was decomposed, this work further analyzes each of its components. Given the utmost relevance of volatility both for financial analysis and practice, this analysis begins with a more detailed study of the noise ξ , later followed by an exploration of the structure of the trend component $\mu(t)$. Note that the seasonality $\lambda(t)$ was obtained by Fourier analysis and is fully determined.

3.3. Factorization of the stochastic component

A preliminary descriptive data analysis of the noise ξ was made, with results shown on Section 4.2. A fact well established in landmark works such as those of Hull and White [7], Stein and Stein [23] or Heston [9], the expected non-normality of ξ is confirmed. A popular approach to deal with this non-normality is to try to consider it as the product of a constant volatility and a stable distribution with

mean 0 and standard deviation 1. Unfortunately, such detours seem to have failed to produce relevant results for practical applications [5]. Therefore, a different approach is used here.

In the proposed generalized model equation (4), it may be possible for ξ to factor as the product of a volatility function $\sigma(t)$ by a noise term. Although, *a priori*, it is not so easy to know whether the combined distribution ξ's heavy tails are caused by large instantaneous volatilities or by outliers of the probability distribution, this work will shed some light on this matter by unveiling both the volatility function's structure and the probability distribution. Indeed, only monthly returns were used in the decomposition of equation (6), despite of having daily data available. By using only monthly data, it is really hard, if possible at all, to separate the volatility function $\sigma(t)$ from the noise and properly factor the aleatory component of the oil prices stochastic process.

Nevertheless, since the relative daily returns were already computed in market data preprocessing, the volatility function can be recovered from daily data as follows: for each month, the number of trading days $n(t)$ can be easily counted, and the month's average daily return $\bar{r}_D(t)$ and the daily volatility $\bar{\sigma}_D(t)$ can be estimated as the daily returns' mean and standard deviation, respectively; the monthly return and volatility can then be computed by the formulae:

$$\tilde{r}(t) = \left(1 + \bar{r}_D(t) - \frac{\bar{\sigma}_D^2(t)}{2}\right)^{n(t)} - 1 \tag{7}$$

$$\tilde{\sigma}(t) = \sqrt{n(t)}\ \bar{\sigma}_D(t) \tag{8}$$

Note that equation (7) makes use of the risk aversion principle, as done by Luenberger [24], to compensate for the corrosion of return by risk on the long run, while equation (8) uses the usual Black–Scholes model of equation (1) as a short-term proxy. These equations will allow for the estimation of each monthly return and risk, respectively, from the corresponding daily parameters, as exhibited on Section 4.3.

The estimated monthly volatility $\tilde{\sigma}(t)$ will then be used to factor the measured aleatory component ξ of the oil prices' stochastic process in order to obtain a realization of the sought noise:

$$R(t) = \frac{\xi}{\tilde{\sigma}(t)} \tag{9}$$

Results of this factorization are shown in Section 4.4, and lead to an improved version of equation (4).

3.4. Stochastic volatility

Once the proposed model has been validated, this work further explores the stochastic structure of the volatility function, $\sigma(t) = \tilde{\sigma}(t)$. Results from Section 4.3 confirm that volatility has a stochastic structure, as already known from works of Hull and White [7], Stein and Stein [23] or Heston [9]. All those works and several others thereafter consider variance itself as an Itô process with constant parameters. Most stochastic volatility models are based in Heston's mean-reversing variance process, which works nicely for stocks but not so well for commodities. Authors such as Doran and Ronn [25],

explains these models unconformity with market reality as “a negative market price of volatility risk” and struggle around it.

This work treats stochastic volatility with a different approach: instead of treating variance itself directly as a stochastic process, a volatility ratio is considered. Similar to stock prices, volatility is always positive and it makes sense to compute the volatility ratio:

$$v_t = \frac{\sigma_t}{\sigma_{t-1}} \tag{10}$$

This equation is analogous to equation (3), except that, when prices are concerned, one is usually interested in the relative return, while, for volatility, the ratio itself tuns out to be more relevant. The resulting monthly volatility ratios are exhibited and treated in Section 4.5, which clarifies the stochastic structure of the volatility, further detailed in Section 4.6.

It is important to mention that the volatility ratio defined in equation (10) differs completely from that used by authors such as Carr and Sun [26], that use ratios between volatilities of different assets. As a matter of fact, the volatility ratio defined in equation (10) is more similar to the one defined by Schwager [27] and commonly used by traders. Notice, however, that Schwager’s volatility ratio does actually compare the period amplitude of prices with the average amplitude of prices over the previous periods, not the volatilities themselves. Nevertheless, the idea is pretty much the same.

3.5. Finite differences of the trend jump process

In order to complete the understanding of the stochastic structure of oil prices, a study of the structure of the trend component $\mu(t)$ is needed. As remarked by Merton [6] and others, the deterministic component of the Black–Sholes price equation may have jumps and other discontinuities. For oil prices, in particular, Fileccia and Sgarra [28] used both stochastic volatility and jumps to better capture the market dynamics. In this work, using the generalized equation (4), this deterministic component was further decomposed into a trend $\mu(t)$ and a seasonal term $\lambda(t)$. Since the seasonal term is a modeled by a continuous finite Fourier series, any jumps must be in the trend term, which may therefore be discontinuous and will be considered here as Wiener process.

Initially, it is necessary to mention that, unlike the expected return of stocks which must always be positive (otherwise no one would be buying), commodities expected returns can be negative. Indeed, commodities can be acquired even by buyers that do believe the price will fall in the near future, provided they need the actual product for immediate consumption. This is clearly the case of oil, as the results of Section 4.1 show.

Now, in an efficient market, expectations about price are formed mostly by the effect of new information that becomes publicly available over current price levels. Thus, in the oil market case, it is reasonable to assume that the variation in expectations is proportional to the difference between the amount of new bullish information and the amount of new bearish information on the time interval considered. Though it is hard to precisely quantify information in terms of its impact on market expectations, the variation of the trend term $\mu(t)$ could be modeled, in terms of probability, by some

sort of a "signed" Poisson distribution that counts the net "quanta" of positive or negative market impact occurring in a time interval. To be more precise, this work treats the finite differences of trend:

$$\Delta\mu = \mu(t+1) - \mu(t) \tag{11}$$

Results for those trend finite differences are shown in Section 4.7, together with a study of their stochastic structure.

3.6. Generalized Moore's transformations

In the exploration of the stochastic structure of the finite differences of trend made is Section 4.7, there is a need to transform the signed Poisson-like distribution considered into normality. To achieve this goal, this work generalizes the transformations defined by Moore [29] so as to be applied to the trend differences. Moore showed that certain usual Poisson processes could be transformed into normality, as using the transformations $M_r: \mathbb{R}_+^* \longrightarrow \mathbb{R}$ given by:

$$M_r(x) = x^r, \quad \text{for any } r \in \mathbb{Q},\ 0 < r < 1. \tag{12}$$

Nevertheless, the trend differences are indeed negative almost half of the time, so that Moore's transformations cannot be directly applied. Thus, it is necessary to extend M_r to $\phi_\alpha: \mathbb{R} \longrightarrow \mathbb{R}$, for any $\alpha > 0$,which can be defined as:

$$\phi_\alpha(x) = \begin{cases} x|x|^{\alpha-1}, & \text{for any } x \neq 0 \\ 0, & \text{if } x = 0 \end{cases} \tag{13}$$

Observe that the functions $\phi_\alpha(x) \equiv M_\alpha(x)$ for any $x > 0$ and any $\alpha \in \mathbb{Q},\ 0 < \alpha < 1$, so that equation (13) directly extends the Moore's transformations of equation (12). Moreover, those functions are continuous, odd and one-to-one. Also note that $\phi_\alpha^{-1} = \phi_{1/\alpha}$.

4. Results

4.1. Time series decomposition of the monthly returns

The seasonal decomposition described in Section 3.2 is shown graphically in FIGURE 3:

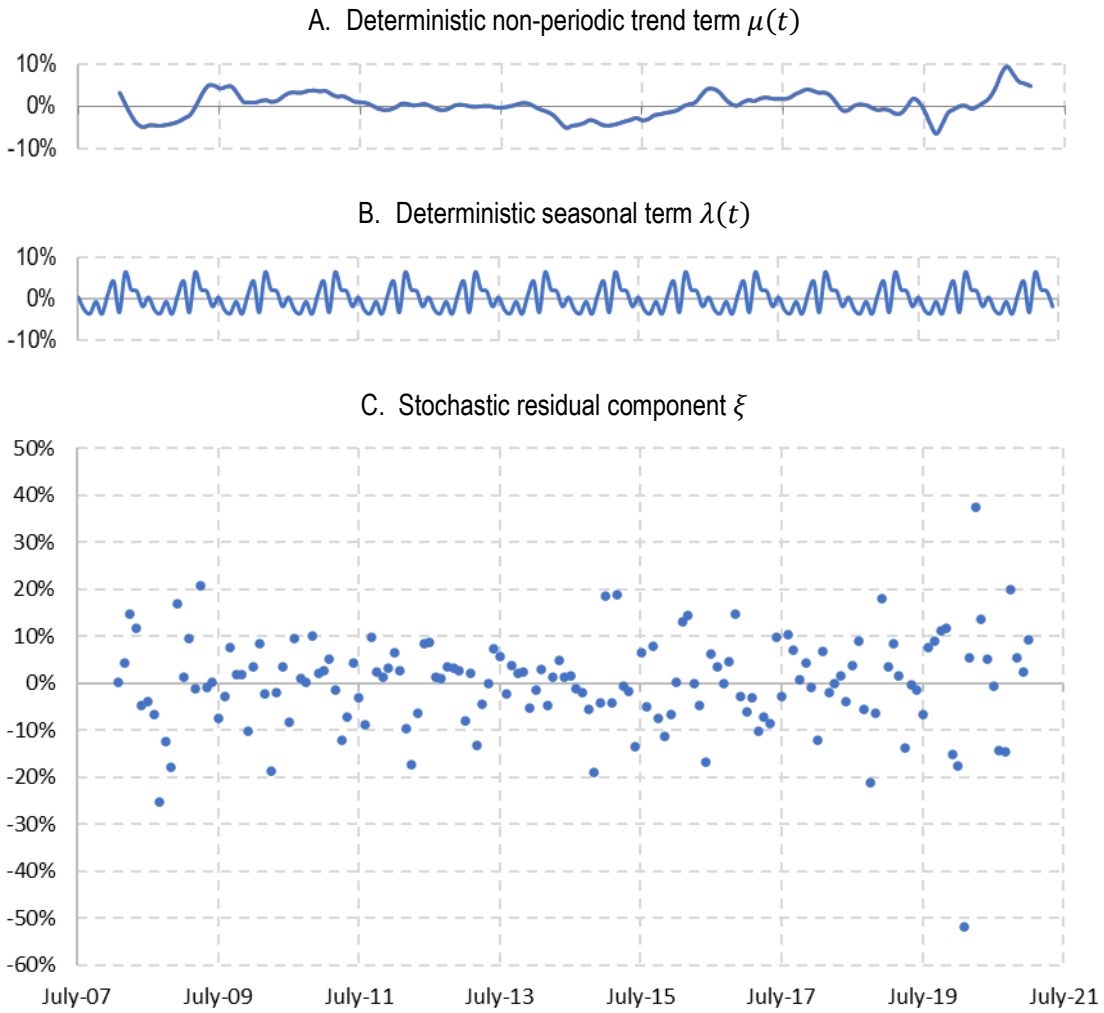

FIGURE 3: Time series additive decomposition for the relative monthly returns of Brent prices, from March 2008 to February 2021, using 12-month centered moving average filtering. (A) Non-periodic trend term of deterministic component. (B) Seasonal term of deterministic component. (C) Residual stochastic component.

Note that the average monthly return throughout this period is $\bar{r} = 0.40\%$, with standard deviation, $s = 10.96\%$. Those are estimations for the usual constant parameters μ and σ, respectively, of traditional Black–Scholes modelling of the oil prices' time series. Using the proposed model decomposition equation (6), estimates for both deterministic functions $\mu(t)$ and $\lambda(t)$ were obtained, with $\bar{\mu} = \bar{r} = 0.40\%$, whereas $\bar{\lambda} = 0.00\%$. Those estimates are graphically shown in FIGURE 3.A and in FIGURE 3.B, respectively. As usual, the deterministic component was smoothed, and so were both its terms, therefore graphed as continuous, smooth curves.

Estimates for the noise term ξ were attained as well, with results shown in FIGURE 3.C, graphed as a dispersion chart, for the stochastic component is intrinsically discontinuous. Note that this chart is similar to FIGURE 2, as the aleatory component of the stochastic process is larger than the deterministic ones. It is important to notice that all graphs in FIGURE 3 share both the same horizontal time frame and the same vertical scale, so that the relative size of the different components can be directly compared. Observe that the stochastic term ξ also has null average. However, its standard deviation is smaller than the traditional Black–Scholes model one obtained earlier. Indeed, $s = 10.12\%$, which is

already an improvement over the traditional model volatility estimation, as s clears the deterministic components' seasonal variations out, allowing for a small noise reduction.

4.2. Probability distribution of the noise

A preliminary data analysis of the stochastic term ξ leads to the histogram shown in FIGURE 4. The computed kurtosis of 4.67 confirms that the distribution is leptokurtic, with heavy tails, while the skewness of -0.68 indicates that the distribution is slightly leaned to the right.

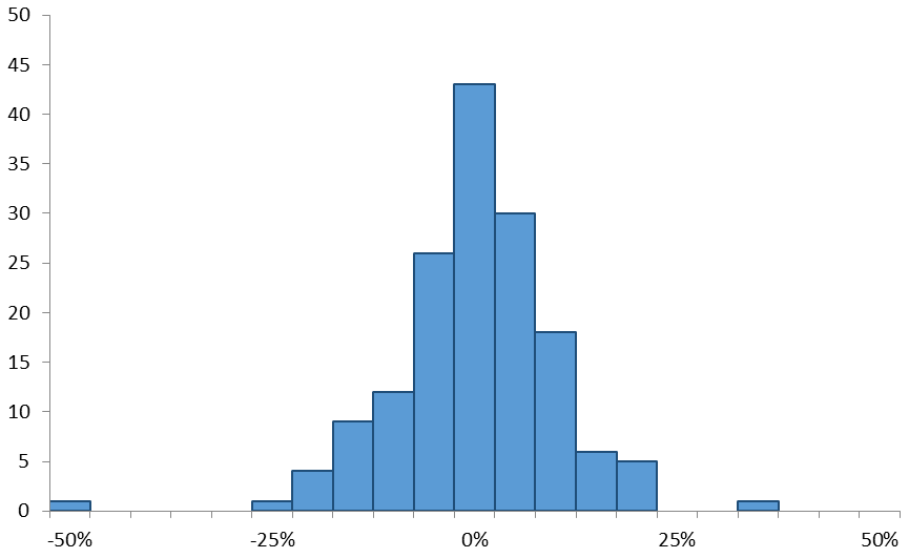

FIGURE 4: Histogram for the residual stochastic component of the relative monthly returns of Brent prices.

The distribution is clearly not normal, a fact confirmed by the Shapiro–Wilk normality test [30], for wich $p = 0.00000930 \ll 0.05$. The non-normality of the stochastic component explains why the traditional Black–Scholes model of equation (1) fails to properly describe the oil prices process.

4.3. Monthly volatility function

Monthly return and risk were estimated from the corresponding daily parameters using, respectively, equations (7) and (8). Note that, although equation (7) is not necessary here, as the actual relative monthly return $r(t)$ is already known from equation (4), comparison between $\tilde{r}(t)$ and $r(t)$, as in FIGURE 5, shows how good this estimation is; indeed, the correlation between actual and estimated values is 99.09%.

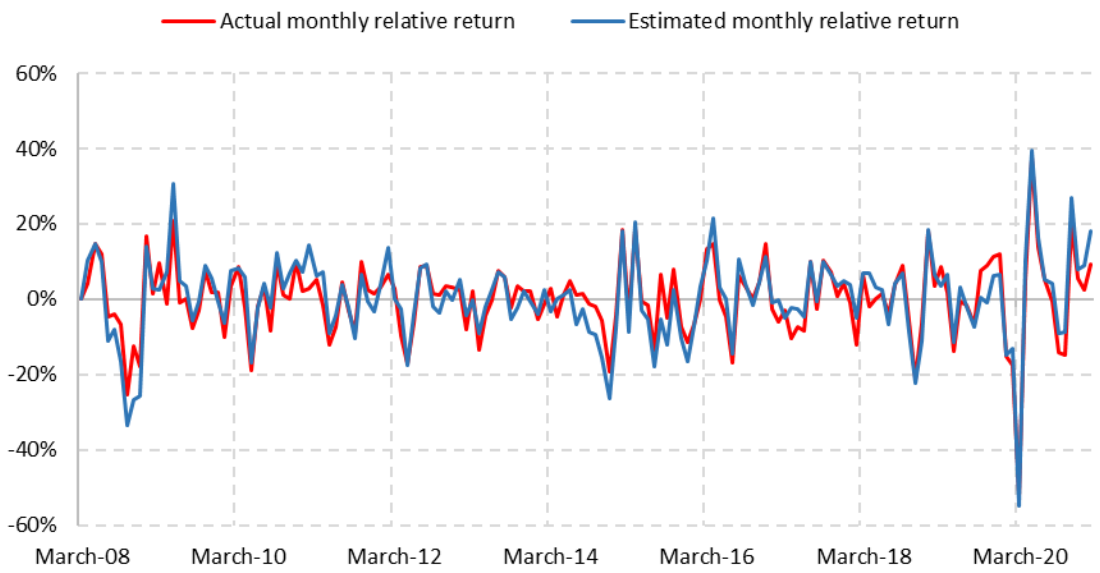

FIGURE 5: Actual and estimated relative monthly returns of Brent prices, from March 2008 to July 2021.

Anyway, the fact that $r(t) \approx \tilde{r}(t)$ shows that equation (7) gives a good estimation for the monthly return and suggests that equation (8) should similarly provide a good estimation for a monthly volatility function. FIGURE 6 shows the monthly volatility $\tilde{\sigma}(t)$ estimated by entering the daily data available into equation (8).

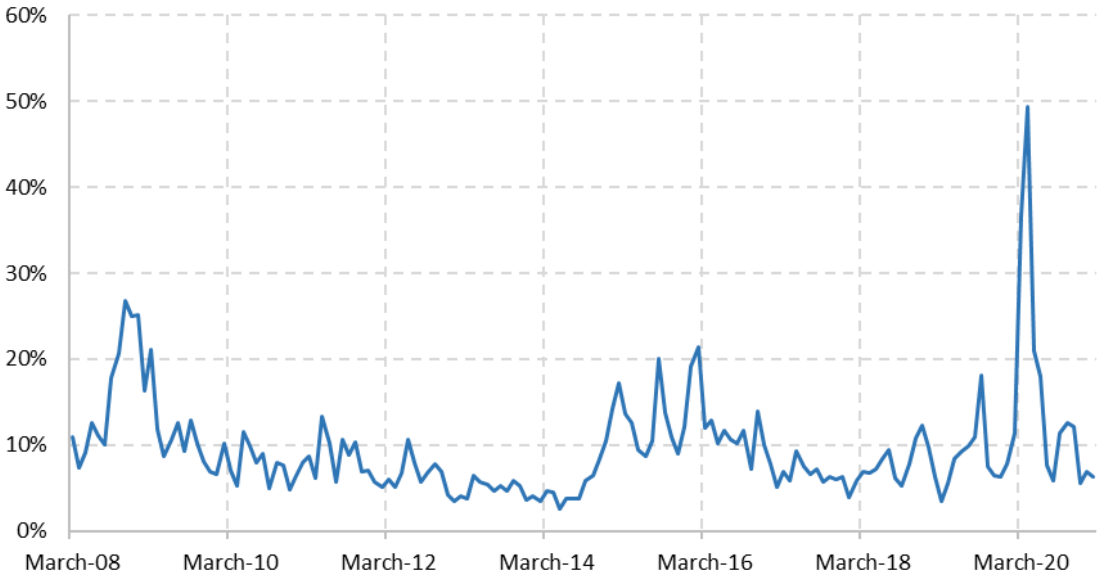

FIGURE 6: Estimated monthly volatility of Brent prices, from March 2008 to July 2021.

4.4. Probability distribution of the residual stochastic component

The monthly volatility function $\tilde{\sigma}(t)$ obtained above is then factored out of the noise ξ of the oil prices by applying equation (9). The corrected residual time series $R(t)$ obtained is graphed in FIGURE 7 as a dispersion chart, and in FIGURE 8 as a histogram.

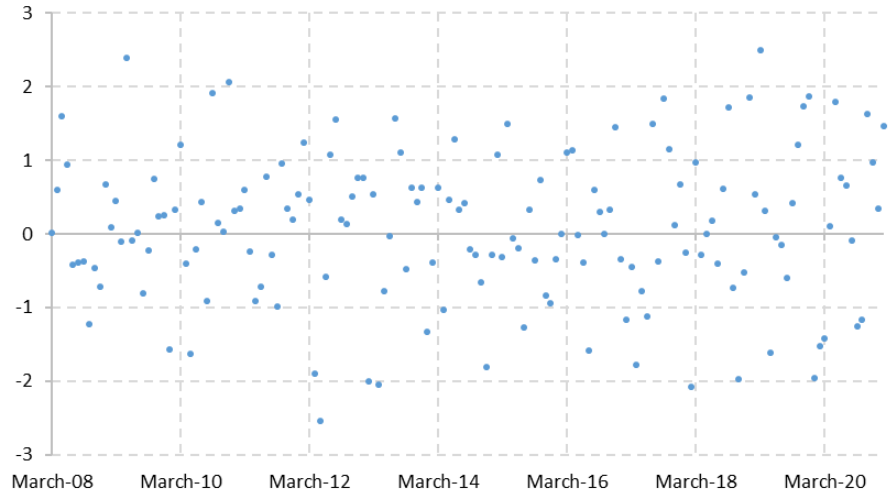

FIGURE 7: Corrected residual stochastic component, from March 2008 to February 2021.

Compare FIGURE 7 to FIGURE 3.C to verify that the outliers in the original residual time series were all properly adjusted by the computed volatility function and are not so extreme anymore. A similar comparison of FIGURE 8 with FIGURE 4 also reinforces this perception, as the heavy tails of ξ are apparently no longer present.

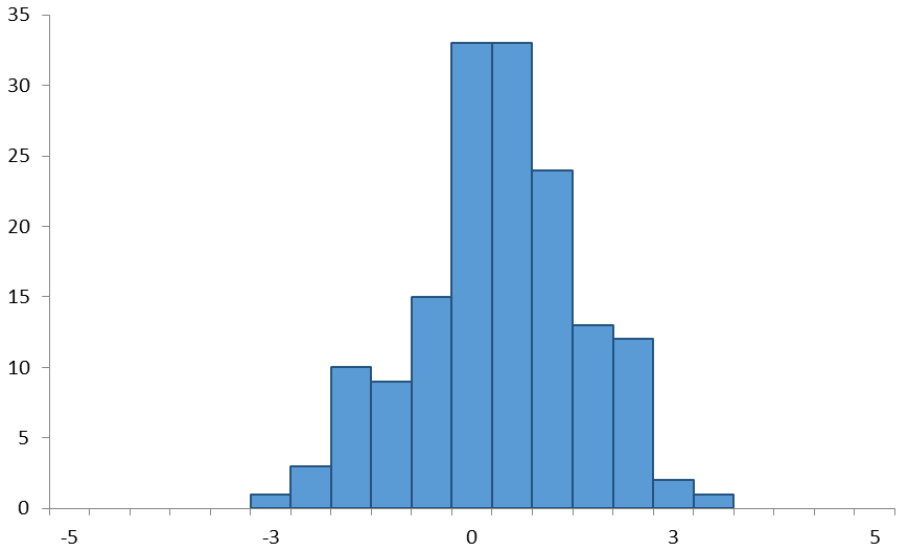

FIGURE 8: Histogram for the corrected residual stochastic component of the relative monthly returns.

From FIGURES 7 and 8 it is easy to notice that $R(t)$ looks much more like a white noise. This visual impression is statistically confirmed by the Shapiro–Wilk normality test [30], for wich $p = 0.48975796 \gg 0.05$. Thus, the corrected residual stochastic component $R(t)$ most likely follows a

normal distribution. Moreover, notice that, since $E[R(t)] = 0.07016$ and $\mathrm{Var}[R(t)] = 1.01917$, it is indeed possible to further factor the noise as $\xi \approx \sigma(t)\,\eta_1$, where $\sigma(t) = \tilde{\sigma}(t)$ and η_1 follows a standard normal distribution.

Thus, on the time span considered, market data confirm that Brent crude oil prices closely follow the proposed generalized Black–Scholes stochastic differential with seasonality, given by equation (4). Results actually show that the oil prices' stochastic process can be simplified to

$$\frac{dP}{P} = [\mu(t) + \lambda(t)]\,dt + \sigma(t)\,\eta_1\,\sqrt{dt}\,. \tag{14}$$

with a white noise η_1 leading randomness in the stochastic component.

4.5. Volatility ratio

To investigate the stochastic structure of volatility, the monthly volatility ratios were computed using equation (10), from March 2008 to February 2021. Results are shown on FIGURE 9 below.

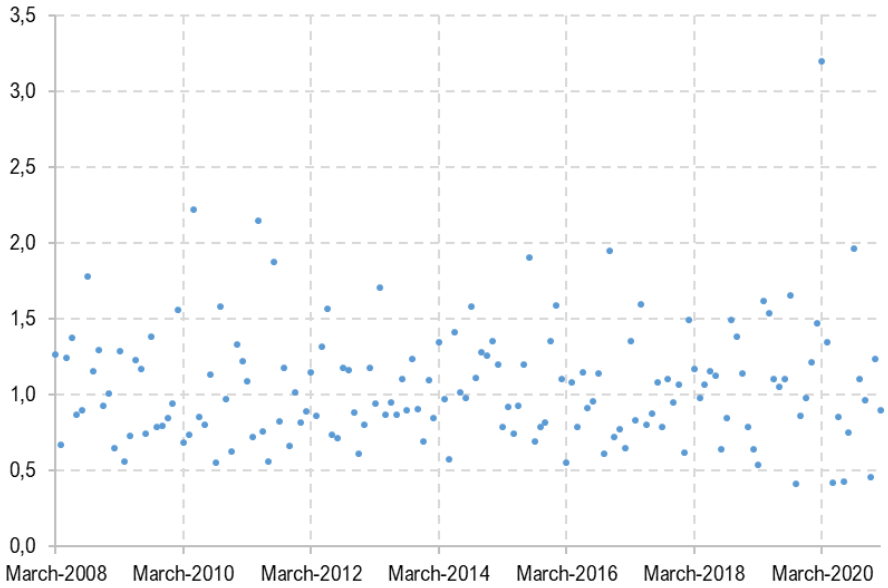

FIGURE 9: Volatility ratio for Brent prices, from March 2008 to July 2021.

Huge outliers can be easily spotted only on the upper half of FIGURE 9, such as those major increases corresponding again to subprime and COVID-19 crises. However, few extreme outliers show up on the lower half of FIGURE 9. While the market gets nervous at once, it calms down slowly. Thus, volatility can increase very fast on extreme situations, but it only comes back down in smaller steps. On its turn, FIGURE 10 shows the corresponding histogram, which has a distinctive lognormal appearance, to be confirmed by normality tests to follow.

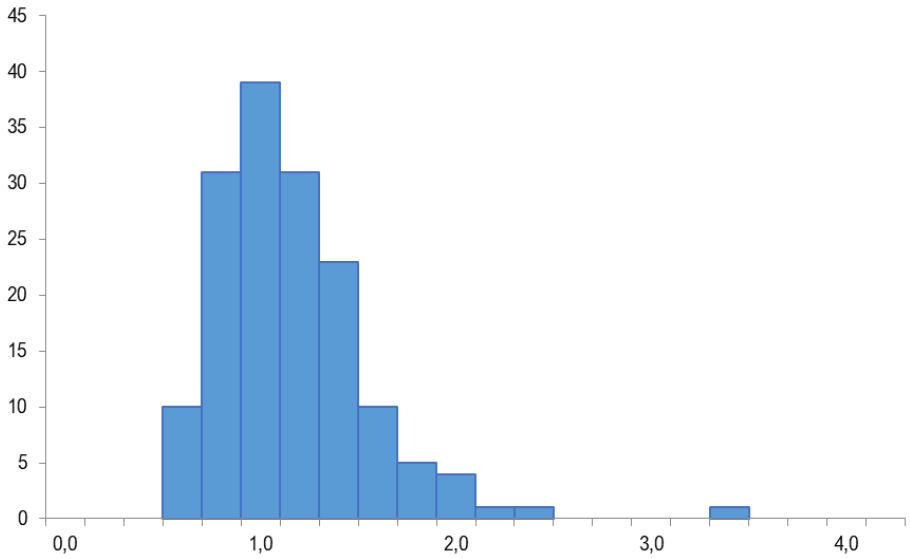

FIGURE 10: Histogram for the volatility ratio for Brent prices, from March 2008 to July 2021.

To achieve normality, the natural logarithm was applied to both sides of equation (10), producing the results shown on FIGURES 11 and 12. It is easy to see that $\ln v_t$ seems to be a normally distributed random variable. This fact is statistically confirmed by the Shapiro–Wilk normality test [30], for wich $p = 0.76034331 \gg 0.05$. Thus, the logarithm of the volatility ratio most likely follow a normal distribution, and the volatility ratio defined in equation (10) indeed has a lognormal distribution.

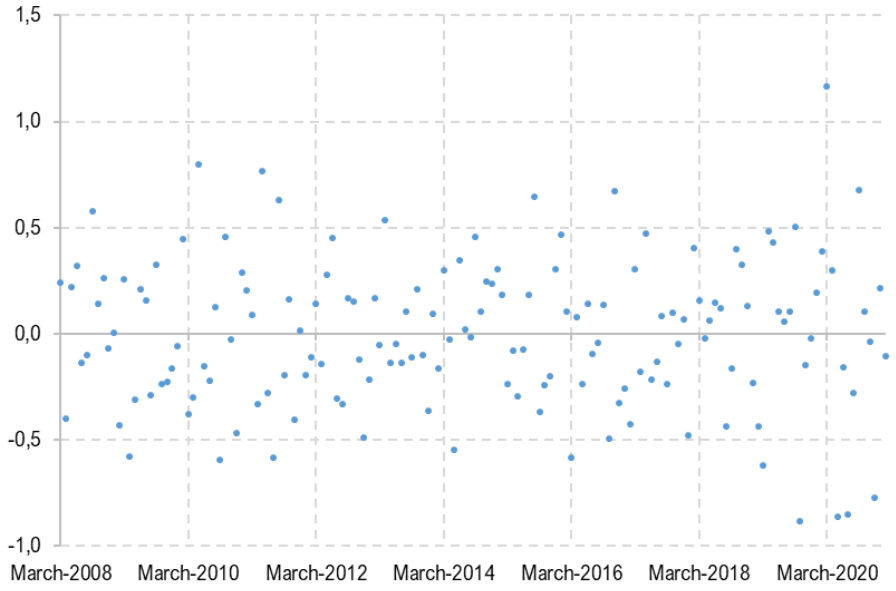

FIGURE 11: Logarithm of volatility ratio for Brent prices, from March 2008 to July 2021.

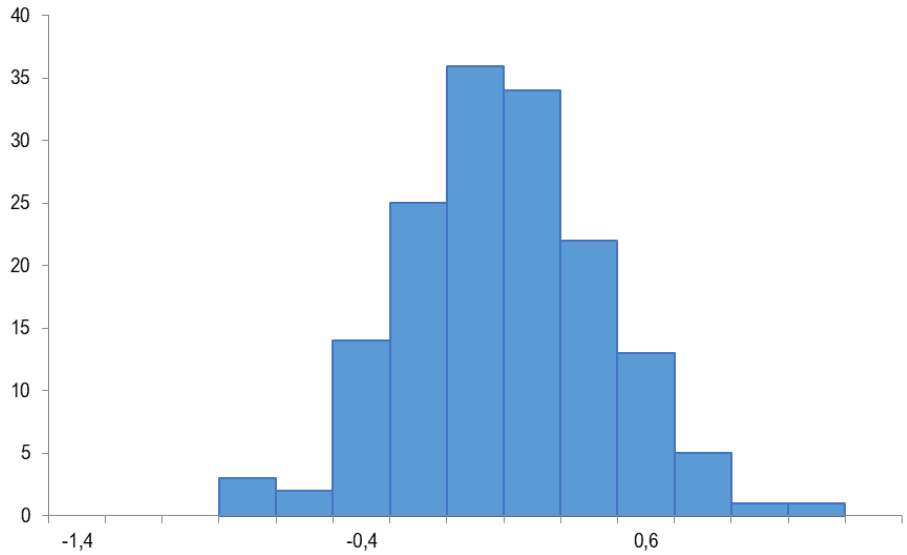

FIGURE 12: Histogram for the logarithm of the volatility ratio for Brent prices, from March 2008 to July 2021.

4.6. Stochastic volatility

From the lognormal volatility ratios, it is possible to infer a stochastic differences' equation for the volatility itself, as follows. Equation (10) can be rewritten as a differences' equation:

$$v_t = \frac{\sigma_t}{\sigma_{t-1}} = \frac{\sigma_{t-1} + \Delta\sigma}{\sigma_{t-1}} = 1 + \frac{\Delta\sigma}{\sigma_{t-1}} \approx 1 + \frac{\Delta\sigma}{\sigma} \tag{15}$$

The lognormal property of volatility ratios, therefore, translates into the equation:

$$\ln\left(1 + \frac{\Delta\sigma}{\sigma}\right) \approx a + b\,\tilde{\eta} \tag{16}$$

where $a = 0.00159531$ and $b = 0.36010702$ are the mean and the standard deviation of the logarithm of the volatility ratios and $\tilde{\eta}$ follows a standard normal distribution.

Applying the exponential function on both side of equation (16), it becomes

$$\frac{\Delta\sigma}{\sigma} \approx \exp(a + b\,\tilde{\eta}\,) - 1 \tag{17}$$

These equations will be very useful for Monte Carlo simulations and other further applications of the model proposed and already validated in this work.

It is important to mention that the $\tilde{\eta}$ from equation (17) and η_1 from equation (14) may be correlated. Indeed, their correlation coefficient is easily computed as $\tilde{\rho}_1 = -0.15641764$. As noted by Fouque, Papanicolaou and Sircar, such a negative correlation between prices and volatility reveals some sort of leverage effect [31]. Proceeding as Drăgulescu and Yakovenko [32], it is convenient to decompose the Wiener process by making

$$\tilde{\eta} = \tilde{\rho}_1.\eta_1 + \sqrt{1 - \tilde{\rho}_1^2}\ \eta_2 \tag{18}$$

where η_2 is another standard Gaussian distribution, uncorrelated to η_1. This decomposition is of paramount importance when running Monte Carlo simulations, as it preserves the correlation structure of the stochastic processes, while taking advantage of the properties of standard normal distributions in generating the random walks.

4.7. Finite differences of the trend jump process

The computed trend finite differences are graphically represented in FIGURE 13, followed by the corresponding histogram, shown in FIGURE 14. As expected for a term from the deterministic component of equation (4), those trend differences are really close to zero $E[\Delta\mu] = -0.00021$ and have a pretty small variance $\mathrm{Var}[\Delta\mu] = 0.00012$. Thus, except for a few isolated jumps here and there, the trend behaves almost like a smooth function. Those scattered jumps, however, can have big impact on prices and cannot be ignored.

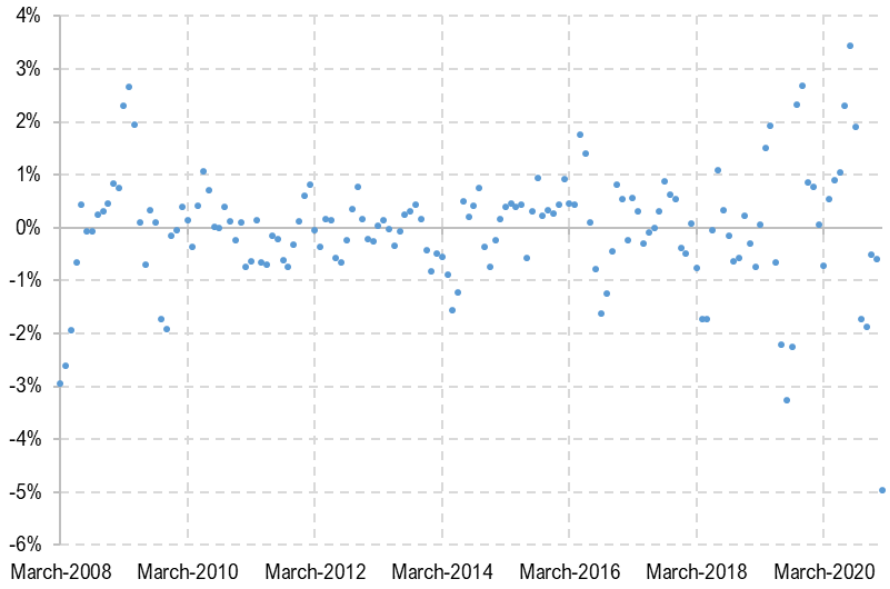

FIGURE 13: Finite differences of trend for Brent prices, from March 2008 to July 2021.

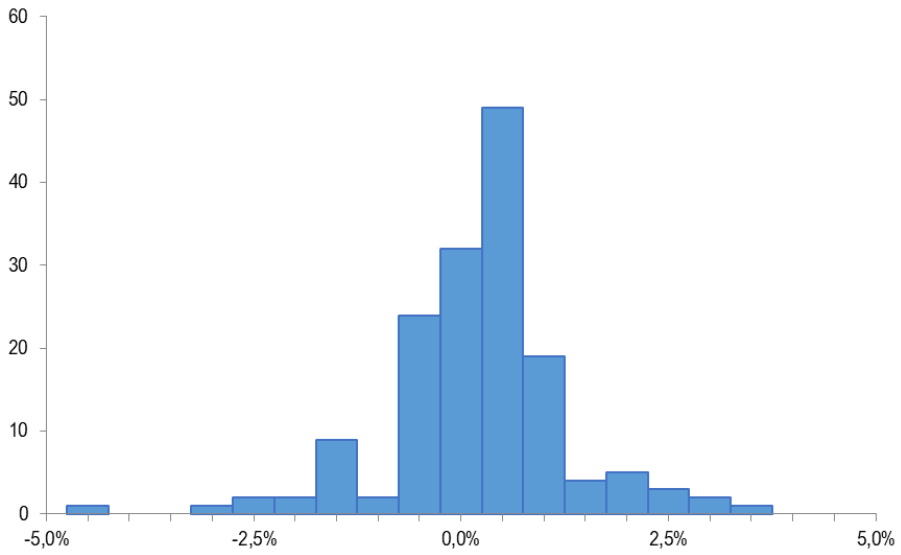

FIGURE 14: Histogram for the finite differences of trend for Brent prices, from March 2008 to July 2021.

Now, applying the extended Moore transformation $\phi_{1/\sqrt{2}}$, obtained from equation (13) with $\alpha = 1/\sqrt{2}$, to the trend differences $\Delta\mu$, the results shown on FIGURES 15 and 16 are obtained.

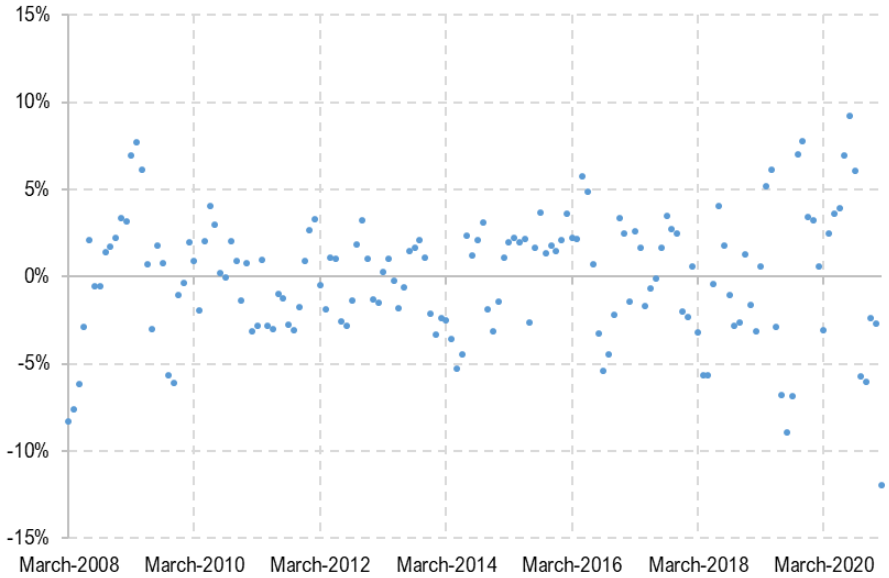

FIGURE 15: Transformation $\phi_{1/\sqrt{2}}$ of the finite differences of trend for Brent prices.

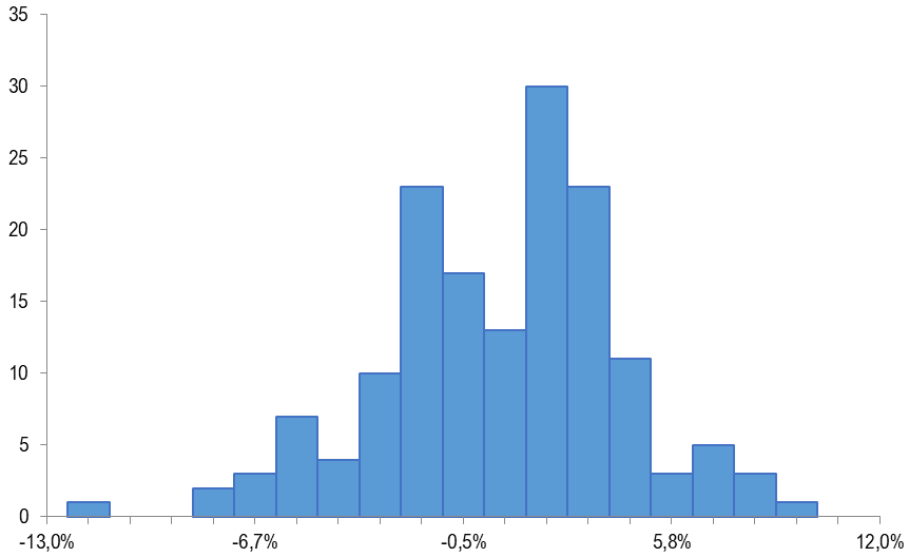

FIGURE 16: Histogram of the transformation $\phi_{1/\sqrt{2}}$ of the finite differences of trend for Brent prices.

Once more, the transformed distribution looks more like the result of a normally distributed random variable, a fact also statistically confirmed by the Shapiro–Wilk normality test [30], for wich $p = 0.09293336 \gg 0.05$. Thus, the trend differences are compatible with an extended Moore transformation of a normal distribution, and the finite differences of trend can be written as

$$\Delta\mu \approx c.\,\phi_{\sqrt{2}}(\check{\eta}) \tag{19}$$

where $c = 0.03548132$ and $\check{\eta}$ is a standard normal distribution. This equation will also be very useful for Monte Carlo simulations and other possible applications of the model proposed in this work.

It is important to mention that the $\check{\eta}$ from equation (19) may be correlated to η_1 and η_2 from equation (18). As a matter of fact, the corresponding correlation coefficients are easy to compute: $\check{\rho}_1 = 0.01799545$ and $\check{\rho}_2 = -0.08847237$. Once again proceeding as Drăgulescu and Yakovenko [32], it is convenient to decompose the Wiener process by making

$$\check{\eta} = \check{\rho}_1.\eta_1 + \check{\rho}_2.\eta_2 + \sqrt{1 - \check{\rho}_1^2 - \check{\rho}_2^2}\ \eta_3 \tag{20}$$

where η_3 is yet another standard Gaussian distribution, uncorrelated to both η_1 and η_2. This decomposition is also important when running Monte Carlo simulations, as it preserves the correlation structure of the stochastic processes and simultaneously takes advantage of the properties of standard normal distributions while generating the random walks.

5. Application

5.1. Markov Chain Monte Carlo simulation

Once the stochastic structure of oil prices has been detailed and validated, it is necessary to find solutions of equation (14). Closed form solutions of such stochastic differential equations may be difficult to obtain, and the use of numerical methods becomes imperative in most practical applications, as noted by Kloeden and Platen [33]. In Finance, in particular, the usage of Monte Carlo methods became an industry standard, both for pricing and risk analysis. The works of Jäckel [34] and Glasserman [35] illustrate several practical financial applications, such as option pricing, interest rates modelling, value at risk estimates and stress tests.

Nevertheless, as mentioned by Platten and Bruti-Liberati [36], the presence of state variables in a stochastic differential equation makes the search for numerical solutions a more complex challenge. This is precisely the case of Black–Scholes models with jumps in expected return and stochastic volatility. Therefore, scholars like Fileccia and Sgarra [28] have being using Markov Chain Monte Carlo simulations for oil prices, and this work does similar simulations, as follows.

A sequence of monthly prices can be produced from combining equations (3) and (14), so as to obtain

$$P_{t+1} = P_t \,.\, (1 + \mu_{t+1} + \lambda_{t+1} + \sigma_{t+1}\, \eta_1) \tag{21}$$

As for the state variables, a sequence of volatilities is taken from a combination of equations (10), (15) and (17) as

$$\sigma_{t+1} = \sigma_t \,.\, \exp(0.00159531 + 0.36010702\, \tilde{\eta}), \tag{22}$$

whereas a sequence of the trend component of the expected return is obtained from equation (19) by

$$\mu_{t+1} = \mu_t + 0.03548132\, \phi_{\sqrt{2}}(\check{\eta}) \tag{23}$$

and the seasonal component of the expected return is determined by $\lambda_{t+12} = \lambda_t$, for $t \in \mathbb{N}$.

The random variables $\tilde{\eta}$ and $\check{\eta}$ are taken directly form equations (18) and (20), respectively. Thus, on each step of the simulation, only uncorrelated realizations η_1, η_2 and η_3 of the standard normal distribution are needed. This allows for faster simulations, as white noise can be easily and quickly random generated.

Since the data considered in this work spans a period ending in July 2021, that month is taken as the starting time of the simulation, $t = 0$. The initial parameters were then set to: $P_0 = 76.33$, the close of that month's last trade day; $\sigma_0 = 0.1005381$ and $\mu_0 = 0.0069$, the monthly volatility and relative return, respectively, computed from daily data of that month using formulae (7) and (8). The seasonal component initial values are show in TABLE 1 bellow and were also shown graphically in FIGURE 3.B.

t	λ_t
0	-0.01853399

1	0.00331504
2	−0.02681545
3	−0.03521763
4	−0.00735258
5	−0.03653946
6	0.00880540
7	0.04173366
8	−0.03274355
9	0.06310797
10	0.02271245
11	0.01752814

TABLE 1: The monthly seasonal component $\lambda(t)$ of Brent prices.

Several simulations were then run for the following 12 months. In each simulation, n sample paths were randomly generated using equations (21), (22) and (23) and the initial parameters just described. In addition, for each month, the percentiles of the price distribution were computed and the time elapsed was recorded.

As for the time consumed in the simulations, on an Intel® Core™ i7-9750H CPU at 2.60 GHz with 16 GB and a NVIDIA GeForce GTX 1050, a reasonably affordable machine, it took an average computing time of 183 μs to generate each sample paths. TABLE 2 below exhibits the time $T(n)$ used up to generate n sample paths in some of the simulations made:

n	$T(n)$
1,000	0.175
5,000	0.896
10,000	1.760
50,000	8.833
100,000	17.894
500,000	92.454
1,000,000	179.742
5,000,000	919.654
10,000,000	1,829.802

TABLE 2: Computing time $T(n)$ in seconds used up to generate n sample paths.

As usual, Monte Carlo simulation time grows linearly with the number of paths randomly generated. Indeed, the linear regression $T = 0.000183\ n$ has a R-squared coefficient of 1.0000.

In terms of convergence, all simulations over 5,000,000 sample paths agree within 1¢ error margin on every percentile, which is good enough for any practical purposes. For as few as 10,000 sample paths, error margins may increase by a factor of 10, but the percentiles quickly converge as $n \to \infty$. Results in TABLE 3 illustrate that convergence for the 1-month median of the generated paths, for a sequence of simulations.

n	$\tilde{P}_1(n)$
1,000	77.04
5,000	77.21
10,000	77.01
50,000	77.13
100,000	77.13
500,000	77.11
1,000,000	77.09
5,000,000	77.11
10,000,000	77.11

TABLE 3: Convergence of the median of 1-month $\tilde{P}_1(n)$ as the number of sample paths n grows.

Selected percentiles for a simulation with $n = 10{,}000{,}000$ are shown in TABLE 4, corresponding to the median, the 1st and 3rd quartiles, and the 1st and 9th deciles for selected months.

p	P_1	P_2	P_6	P_{12}
10	66.08	59.31	43.47	37.24
25	71.88	67.54	56.88	55.73
50	77.11	75.04	69.56	75.62
75	81.94	82.06	81.40	94.03
90	86.68	89.38	95.30	116.79

TABLE 4: Selected percentiles p for Markov Chain Monte Carlo simulation at $t = 1, 2, 6$ and 12 months. Oil prices are expressed in USD / bbl.

The results of TABLE 4 are among the ones shown graphically in FIGURE 17, which shows those and a few more selected percentiles for every month in the simulation. Some of these results will be used next for value at risk estimates.

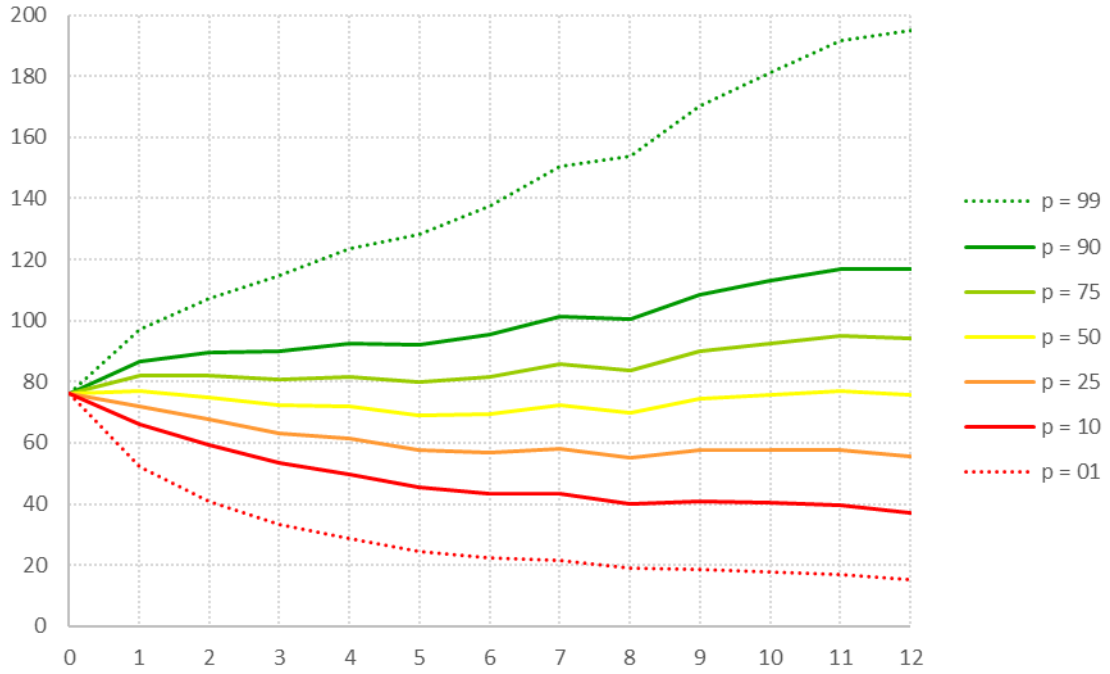

FIGURE 17: Selected percentiles p for Markov Chain Monte Carlo simulations. Oil prices are expressed in USD / bbl and time is shown in months.

5.2. Value at Risk for a Brent oil physical hedge

For an application of the Markov Chain Monte Carlo simulations produced in this work, consider a company that runs a power plant that buys oil on a regular basis for energy production. By the end of July 2021, that company had to decide whether to hedge against a possible increase in oil prices or not. A physical hedging could easily be done, buying oil at the spot price of 76.33 USD / bbl and storing it for 0.50 USD / bbl until it is needed to generate power in September, thus protecting the company from unexpected increases in oil prices, and ensuring the oil supply for that month.

Such an operation bears capital and storage costs but eliminates the risk of financial losses from higher prices. Thus, should oil price rise in August, say, to 80.00 USD / bbl, the company would have a financial gain of 3.17 USD / bbl. However, that company is still subject to market risk due to decreasing prices, as it would be cheaper to buy the necessary oil at the spot market by the end of that month, should the price fall or even increase a little bit in August. In this case, the hedge operation would result in a financial loss for the company.

The risk of bearing such a loss is usually measured in terms of value at risk, using a methodology introduced in the 1990's by risk analysts from J. P. Morgan. According to Jorion's definition, given a confidence level and a time horizon, the value at risk of an investment should be the maximum financial loss that would be incurred therein [37]. The value at risk is usually expressed in currency nominal value or in terms of relative return, but any other relevant, meaningful, measurable way is also acceptable.

For instance, the 1-month 90% value at risk for the hedging operation above can be computed by estimating the minimum financial loss if prices fall into the 1st decile. From TABLE 4, for $p = 10$, the corresponding 1-month minimum price is $66.08\ \text{USD} / \text{bbl}$, with only a probability of 10% of the price falling below that mark. Hence, with interest rates set aside, the desired value at risk is given by

$$90\%\ \text{VaR}_{1-\text{month}} = 76.33\ \text{USD} / \text{bbl} + 0.50\ \text{USD} / \text{bbl} - 66.08\ \text{USD} / \text{bbl} = 10.75\ \text{USD} / \text{bbl}$$

Graphically, this is the financial loss the company would suffer, if the oil price ended up August on the red line of FIGURE 17. By the end of August 2021, the actual market price for Brent oil was $72.99\ \text{USD} / \text{bbl}$, so that this value at risk estimate was not breached in that month, i.e., the red line was not crossed.

Similarly, the 1-month 75% value at risk would use the 1st quartile. Again, from TABLE 4, for $p = 25$, the corresponding 1-month minimum price is $71.88\ \text{USD} / \text{bbl}$, with a 75% probability. The value at risk becomes

$$75\%\ \text{VaR}_{1-\text{month}} = 76.33\ \text{USD} / \text{bbl} + 0.50\ \text{USD} / \text{bbl} - 71.88\ \text{USD} / \text{bbl} = 4.95\ \text{USD} / \text{bbl}$$

Again, this is the financial loss the company would incur in, should the oil price finished August on the orange line of FIGURE 17. This value at risk estimate was not breached either, i.e., the orange line was not touched either. Note that the value at risk estimate for September 2021 were not breached either, as the price actually increased to $78.52\ \text{USD} / \text{bbl}$ during that month, and neither the red nor the orange lines of FIGURE 17 were crossed.

6. Conclusion

Market data from Brent crude oil contracts validate the proposed stochastic structure for oil prices, confirming that the Brent prices closely follow a generalized Black–Scholes equation

$$\frac{dP}{P} = [\mu(t) + \lambda(t)]\, dt + \sigma(t)\, \eta\, \sqrt{dt}\,. \tag{24}$$

where η follows the standard normal distribution. This provides an improved understanding of the stochastic behavior of oil prices.

The components of the deterministic term of equation (24), discontinuous trend $\mu(t)$ and periodic $\lambda(t)$, were obtained by smoothing and harmonic analysis, in a usual time series decomposition, while the stochastic volatility function $\sigma(t)$ was accessed by rescaling time from a finer daily grid. The stochastic volatility ratio was determined to follow a lognormal distribution, whereas the jumps in trend were modeled by a normal distribution under a generalized More transformation.

The results for Brent crude oil prices are so good that the proposed generalized model equation (24) can be confidently used in several practical applications, such as risk analysis or derivative pricing. The decomposition obtained in this work may bring new light to the study of oil prices and allow for

improved practical applications in the crude oil market. In order to illustrate that, some Markov Chain Monte Carlo simulations were run and the results used to produce value at risk estimates for a physical hedging operation.

Further developments

A straightforward development is to verify the validity of the generalized model for several other commodities, as well as for other kinds of assets, e.g., small caps, for which traditional Black–Scholes model does not perform well. Another possible way to improve the model accuracy is to refine estimations of functions $\mu(t)$, $\lambda(t)$ and $\sigma(t)$ by using a finer, intraday data set.

It is also desirable to better understand the relation of $\mu(t)$ with major macroeconomic parameters, such as interest rates, economic and population growth, as well as with major microeconomic oil sector indicators, such as demand, convenience yield and storage fees. Similarly, it is important to study the relation of $\lambda(t)$ with major oil demand drivers. Even more important is to isolate the major uncertainty factors that impact the volatility $\sigma(t)$, and to understand how they affect variations of this function.

Finally, the Markov Chain Monte Carlo simulations can be applied to several other situations in the oil market, such as the pricing of exotic options. These simulations can also be much faster, by using parallel computing on faster machines, allowing perhaps for real time pricing and analysis.

CRediT authorship contribution statement

Leopoldo Grajeda: conceptualization, data curation, formal analysis, investigation, methodology, software, validation, visualization, writing – original draft. **José Roberto Steiner:** project administration, formal analysis, validation, writing – review and editing. **Raphael Lima:** conceptualization, fund acquisition, investigation, resources, supervision.

Declaration of competing interests

The authors report financial support provided by GAVB Consulting (Boticario Group), from Canoas, RS, Brazil.

Acknowledgements

The authors are thankful to Prof. Dr. Allbens Atman from CEFET-MG for proofreading this work, to Prof. Dr. Lourdes Montenegro from UFMG for her assistance with normality tests, and to Dr. Christiano Maia from DRW for his insights about the oil market. Their comments and suggestions surely improved the quality of this work. It is also important to thank Dr. Domingos Santos Jr. and Dr.

Felipe Minuzzi, both from GAVB Consulting, for their help with the Python programming of the statistical methods used here. As a final recognition, the authors acknowledge the financial support of GAVB Consulting (Boticario Group), from Canoas, RS, Brazil.

References

[1] Bachelier, L.: Théorie de la Spéculation. *Annales Scientifiques de l'École Normale Supérieure. 3e. Série,* **17**, pp. 21-86 (1900)

[2] Einstein, A.: Über die von der molekularkinetischen Theorie der Wärme geforderte Bewegung von in ruhenden Flüssigkeiten suspendierten Teilchen. *Annalen der Physik,* **322** (8), pp. 549-560 (1905)

[3] Itô, K.: On Stochastic Differential Equations. *Memoirs of the American Mathematical Society,* **4**, 1-51 (1951)

[4] Black, F., Scholes, M.: The Pricing of Options and Corporate Liabilities. *Journal of Political Economy*, **81** (3), pp. 637-654 (1973)

[5] Haug, E. G., Taleb, N. N.: Option Traders Use (Very) Sophisticated Heuristics, Never the Black–Scholes–Merton Formula. *Journal of Economic Behavior & Organization,* **77** (2), pp. 97-106 (2011)

[6] Merton, R. C.: Option Pricing when Underlying Sock Returns are Discontinuous. *Journal of Financial Economics,* **3** (1-2), pp. 125-144 (1976)

[7] Hull, J., White, A.: The Pricing of Options on Assets with Stochastic Volatilities. *The Journal of Finance,* **42** (2), pp. 281-300 (1987)

[8] Garman, M. B., Kohlhagen, S. W.: Foreign Currency Option Values. *Journal of International Money and Finance,* **2** (3), pp. 231-237 (1983)

[9] Heston, S. L.: A Closed-Form Solution for Options with Stochastic Volatility with Applications to Bond and Currency Options. *The Review of Financial Studies,* **6** (2), pp. 327-343 (1993)

[10] Cox, J. C., Ingersoll Jr., J. E., Ross, S. A.: The Relation Between Forward Prices and Futures Prices. *Journal of Financial Economics,* **9** (4), pp. 321-346 (1981)

[11] Beckers, S.: On the Efficiency of the Gold Options Market. *Journal of Banking & Finance,* **8** (3), pp. 459-470 (1984)

[12] Schwartz, E.: The Stochastic Behavior of Commodity Prices: Implication for Valuation and Hedging. *The Journal of Finance*, **52** (3), pp. 923-973 (1997)

[13] bp: *Statistical Review of World Energy.* 70 ed. bp, London (2021)

[14] Hunt, L. C., Ninomiya, Y.: Unravelling Trends and Seasonality: A Structural Time Series Analysis of Transport Oil Demand in the UK and Japan. *The Energy Journal,* **24** (3), pp. 63-96 (2003)

[15] Pindyck, R.S.: The Dynamics of Commodity Spot and Futures Markets – A Primer. *The Energy Journal*, **22** (3), pp. 1-29 (2001)

[16] Hamilton, J.D.: Understanding Crude Oil Prices. *The Energy Journal*, **30** (2), pp. 179-206 (2009)

[17] Kolodziej, M., Kaufmann, R.K., Kulatilaka, N., Bicchettic, D., Maystre, N.: Crude oil – commodity or financial asset? *Energy Economics*, **46**, pp. 216-223 (2014)

[18] Byun, S.J.: Speculation in Commodity Futures Markets, Inventories and the Price of Crude Oil. *The Energy Journal*, **38**, (5), pp. 93-117 (2017)

[19] Arismendi, J.C., Back, J., Prokopczuk, M., Paschke, R., Rudolf, M.: Seasonal Stochastic Volatility – Implications for the pricing of commodity options. *Journal of Banking & Finance*, **66**, pp. 53–65 (2016)

[20] Choi, J., Kwak, M., Tee, C. W., Wang, Y.: *A Black-Scholes User's Guide to the Bachelier Model,* s.l.: Preprint submitted to arXiv (2021)

[21] Yahoo! Finance (2019–2021):: *Yfinance* (Version 0.1.59) [Computer software]. https://finance.yahoo.com/

[22] Statsmodels Developers (2009–2021): *Statsmodels* (Version 0.12.0) [Computer software]. https://www.statsmodels.org/

[23] Stein, E.M., Stein, J.C.: Stock Price Distributions with Stochastic Volatility: An Analytic Approach. *The Review of Financial Studies*, **4** (4), pp. 727-752 (1991)

[24] Luenberger, D.: *Investment Science.* 1 ed. New York: Oxford (1997)

[25] Doran, J.S., Ronn, E.I.: Computing the market price of volatility risk in the energy commodity markets. *Journal of Banking & Finance*, **32** (12), pp. 2541-2552 (2008)

[26] Carr, P., Sun, J.: A new approach for option pricing under stochastic volatility. *Review of Derivatives Research*, **10**, pp. 87–150 (2007)

[27] Schwager, J.D.: *Technical Analysis*. New York: John Wiley & Sons, Inc. (1996)

[28] Fileccia, G., Sgarra, C.: A particle filtering approach to oil futures price calibration and forecasting. *Journal of Commodity Markets*, **9**, pp. 21-34 (2018)

[29] Moore, P.G.: Transformations to Normality Using Fractional Powers of the Variable. *Journal of the American Statistical Association*, **52** (278), pp. 237-246 (1957)

[30] Shapiro, S. S., Wilk, M. B.: An Analysis of Variance Test for Normality (Complete Samples). *Biometrika*, **52** (3-4), pp. 591-611 (1965)

[31] Fouque, J. P., Papanicolaou, G., Sircar, K.R.: Derivatives in Financial Markets with Stochastic Volatility. *International Journal of Theoretical and Applied Finance*, 3, pp. 101-142 (2000).

[32] Drăgulescu, A.A., Yakovenko, V.M.: Probability distribution of returns in the Heston model with stochastic volatility. *Quantitative Finance*, **2** (6), pp. 443-453 (2002)

[33] Kloeden, P.E., Platten, E.: *Numerical Solution of Stochastic Differential Equations.* 3 ed. New York: Springer (1992)

[34] Jäckel, P.: *Monte Carlo Methods in Finance*. 1 ed. New York: John Wiley & Sons (2002)

[35] Glasserman, P.: *Monte Carlo Methods in Financial Engineering*. 1 ed. New York: Springer (2003)

[36] Platten, E., Bruti-Liberati, N.: *Numerical Solution of Stochastic Differential Equations with Jumps in Finance.* 3 ed. New York: Springer (2010)

[37] Jorion, P.: *Value at Risk: The New Benchmark for Managing Financial Risk*. 3 ed. New York: McGraw-Hill (2006)